

# TEIPP-vaccination in checkpoint-resistant non-small cell lung cancer: a first-in-human phase I/II dose-escalation study

---

Received: 10 February 2025

---

Accepted: 16 May 2025

---

Published online: 28 May 2025

---

 Check for updates

---

---

A list of authors and their affiliations appears at the end of the paper

---

Functional loss of the intracellular peptide Transporter associated with Antigen Processing (TAP) fosters resistance to T-cell based immunotherapy. We discovered the presentation of an alternative set of shared tumor antigens on such escaped cancers and developed a LRPAP1 synthetic long peptide vaccine (TEIPP24) to stimulate T-cell immunity. In this first-in-human multicenter dose-escalation study with extension cohort, HLA-A\*0201-positive patients with non-small cell lung cancer progressive after checkpoint blockade were treated with TEIPP24 (NCT05898763). Dose escalation followed an adapted 3 + 3 scheme where in each cohort six patients received the TEIPP24 peptide emulsified in Montanide ISA-51 at either 20, 40, 100 µg of peptide, subcutaneously injected three times every three weeks in alternating limbs. The extension cohort of six patients received the highest safe dose of TEIPP24 combined with the PD-1 checkpoint blocker pembrolizumab. The primary objectives of the study were safety, tolerability and immunogenicity of the TEIPP24 vaccine. Secondary objectives included the evaluation of specificity and immune modulatory effects of the vaccine, antigen and immune status of the patients, progression free (PFS) and overall survival (OS) and radiological tumor response rate and duration. A total of 26 patients were enrolled across 2 institutions. Treatment was well tolerated, and vaccine-induced LRPAP1-specific CD8<sup>+</sup> T cells were detected in 20 of 24 evaluable patients (83%). In 13 of 21 tested cases (62%) vaccine-specific CD4<sup>+</sup> T cells were also detected. The increase in activated polyfunctional CD8<sup>+</sup> effector T cells was influenced by vaccine dose, number of vaccines administered, induction of a CD4<sup>+</sup> T-cell response, and the pre-existing frequency of monocytic cells. Co-administration of pembrolizumab resulted in the ex-vivo detection of activated (HLA-DR<sup>+</sup>, PD-1<sup>+</sup>, ICOS<sup>+</sup>) LRPAP1-specific CD8<sup>+</sup> T cells. The observation of one PR, 8 stable diseases and 2 mixed responses in 24 evaluable patients after vaccination, correlated with a stronger vaccine-induced CD8<sup>+</sup> T-cell response to this single epitope from this new class of cancer antigens.

Immunogenic tumors can be controlled by tumor-reactive CD8<sup>+</sup> T cells either directly or after checkpoint blockade. In the end, most tumors acquire resistance mechanisms and escape immune control<sup>1,2</sup>. One such mechanism is the down regulation of intracellular peptide

Transporter associated with Antigen Processing 1 and 2 heterodimer (TAP1, TAP2). TAP downregulation is observed frequently in cancer, including lung cancer, melanoma, colorectal cancer, head and neck cancers, and prostate cancer. All for which (partial) downregulation of

TAP1 and/or TAP2 was reported in at least half of the tumors analyzed<sup>3–8</sup>. TAP downregulation results in the impaired presentation of conventional (neo)antigens in HLA class I and evasion from tumor-reactive CD8<sup>+</sup> T cell mediated control. The importance of this is well-illustrated by the correlation between TAP defects and worse clinicopathological parameters as well as loss of durable benefit to checkpoint blockade therapy<sup>9,10</sup>.

We previously identified a new class of tumor antigens known as T-cell Epitopes associated with Impaired Peptide Processing (TEIPP) and showed that by focusing the T-cell response towards this novel set of ubiquitous, nonmutated and immunogenic self-antigens, it is possible to safely reinstall effective tumor-immunity to cancers displaying TAP-defects in preclinical models<sup>11–13</sup>. Subsequently, we identified a human TEIPP in the ubiquitously expressed protein LRPAP1. This LRPAP1-TEIPP is able to activate HLA-A\*0201-restricted LRPAP1<sub>21–30</sub>-specific CD8<sup>+</sup> T-cells that preferentially recognize a series of TAP-impaired tumor cells while remaining unresponsive to healthy cells of the same tissue type<sup>14</sup>. In order to stimulate LRPAP1-TEIPP-specific immunity in patients we developed a vaccine based on the highly immunogenic and clinically successful synthetic long peptide (SLP) platform<sup>15,16</sup>. The LRPAP1<sub>7–30V</sub>-SLP, in which the last serine was replaced by a valine to allow for cross-presentation by dendritic cells (LRPAP1<sub>7–30V</sub>-SLP), was shown to stimulate CD8<sup>+</sup> T cells able to specifically recognize HLA-A\*0201-positive, LRPAP1-positive and TAP-defective tumor cells<sup>17</sup>.

First-line treatment of patients with advanced non-small cell lung cancers (NSCLCs) in the absence of targetable aberrations consists of PD-(L)1 checkpoint inhibition monotherapy or in combination with chemotherapy, depending on PD-L1 expression and the patient's condition. Despite encouraging results of this therapy, only 20–30% of patients with NSCLC experience durable clinical benefit<sup>18</sup>. Lowered expression of TAP1 (25% of cases)<sup>19</sup> and TAP2 (80% of cases)<sup>8</sup> is prominent in NSCLC and points at the potential of TEIPP-specific T cells to aid in the anti-tumor response.

The aim of this first-in-human study was to determine the safety, tolerability and immunogenicity of LRPAP1<sub>7–30V</sub>-SLP admixed with Montanide ISA51 (TEIPP24 vaccine) in patients with NSCLC failing first-line treatment. Secondary endpoints included the radiological tumor response, progression free survival (PFS) and overall survival (OS), all up to one year after first vaccination.

## Results

### Patient population

In total 81 patients with stage IV NSCLC were screened, 33 of whom displayed the correct HLA-A\*0201 type. Ultimately, a total of 26 patients were included in the study and received the TEIPP24 vaccine (Fig. S1). General patient characteristics at baseline are displayed in Table 1. The ratio of men versus women was 1.36 and the median age was 64 years (range 47–79 years) at time of inclusion. Smoking history of patients showed 65% of current smokers, 31% of former smokers and 4% of never smokers. The histological subtypes of the primary tumors were mostly non-small cell adenocarcinomas (58%) and squamous cell carcinomas (35%). All patients received prior immunotherapy (median 7.5 cycles) and all displayed disease progression on CT scans before inclusion. The median interval between administration of the last immunotherapy cycle and initiation of TEIPP24 vaccination was 11 weeks (range 2–54 weeks). Three cohorts of patients received increasing doses of peptide per cohort (i.e. 20, 40, and 100 µg), and cohort 4 received 100 µg of TEIPP24 peptide together with 3 doses of pembrolizumab. To reach the primary endpoint of immunogenicity one extra patient was added to cohorts 2 and 3, because of low PBMC yield in both cohorts. LRPAP1 expression was detected in all of the 22 archival pre-treatment tumor blocks available (Table S1), of which 17 were obtained before patients were treated with first line checkpoint therapy. Deregulated HLA class I and/or TAP expression was observed in 14 of the 20 tumor blocks tested (Table S1).

### Treatment characteristics, safety and tolerability

Of the 26 patients, 23 completed the full vaccination protocol of three injections, the others received two vaccinations (Table 2). Vaccination against the ubiquitously expressed LRPAP1 protein did not result in dose limiting toxicity (DLT). A total of 23 serious adverse events (SAEs) occurred in nine patients, mostly due to disease related hospitalization, and included acute renal impairment, dyspnea, increased CRP, pain and dysphagia. These SAE's were unlikely to be related to the study medication, but ascribed to the underlying malignancy. Initial assessment of the SAE pulmonary embolism, anorexia and hypoxemia did meet criteria for DLT but were reevaluated by the study team and Data Safety Monitoring Board (DSMB) as being associated with disease progression. In total, 35 adverse events (grade 1 or 2, NCI-CTCAE, version 5) were reported to be (possibly) related to the TEIPP24 vaccination (Table 3, Tables S2–S5). Most frequent were malaise ( $n = 4$ ), myalgia ( $n = 4$ ) and pruritis ( $n = 4$ ). Thus, targeting this new class of tumor antigens by therapeutic vaccination does not result in DLT at the dosages tested.

### Therapeutic TEIPP vaccination induces CD8<sup>+</sup> effector T cells

The CD8<sup>+</sup> T cell response to the HLA-A\*0201-restricted LRPAP1<sub>21–30</sub>-peptides was measured in peripheral blood mononuclear cells (PBMC) of 24 patients using a dual MHC dextramer staining in order to make a distinction between CD8<sup>+</sup> T cells responding to the altered peptide ligand LRPAP1<sub>21–30V</sub>, the wild-type peptide LRPAP1<sub>21–30S</sub> and to both (Figure S2a,b). In two patients this analysis could not be performed due to low PBMC yield. As a control, a reference sample comprising endogenous influenza- and CMV-specific HLA-A\*0201-restricted CD8<sup>+</sup> T cells as well as a fixed percentage of HLA-A\*0201-restricted LRPAP1<sub>21–30</sub>-specific T-cell receptor transgenic CD8<sup>+</sup> T cells was taken along at each measurement of a patient sample. This revealed that the tests were highly reproducible, not only with respect to the detection of the responses to influenza ( $0.745\% \pm 0.042\%$ ; CV = 5.6%) and CMV ( $0.035\% \pm 0.011\%$ ; CV = 30%) but also to LRPAP1<sub>21–30</sub> ( $0.536\% \pm 0.059\%$ ; CV = 11%) (Fig. S2c, d).

No vaccine-induced LRPAP1<sub>21–30</sub>-specific CD8<sup>+</sup> T cells were detected directly ex-vivo in cohorts 1–3. In cohort 4, where the vaccine was combined with pembrolizumab such direct ex-vivo responses were detected after vaccination in three out of six patients (Fig. S3). After one round of in vitro expansion, LRPAP1<sub>21–30</sub>-specific CD8<sup>+</sup> T cells were detected in 23 out of 24 patients, and in 19 of these 23 the response was increased after vaccination (Fig. 1a, Table S6). After vaccination, LRPAP1<sub>21–30</sub>-specific CD8<sup>+</sup> T cells stained positive with LRPAP1<sub>21–30S</sub> multimers, indicating their capacity to recognize the wild-type peptide (Fig. S2).

In general, the size of the LRPAP1<sub>21–30</sub>-specific CD8<sup>+</sup> T-cell population increased after each vaccination, especially in cohorts 3 and 4 receiving the highest vaccine dose (Fig. 1b). In addition, the quality of the response changed with the number of vaccinations and dose level. An increase in the percentage of LRPAP1<sub>21–30</sub>-specific CD8<sup>+</sup> effector T cells expressing several proteins associated with TCR-mediated activation (HLA-DR, PD-1, ICOS) was observed. This was most evident after 2–3 vaccinations and in patients receiving the highest vaccine dose (Fig. 1c, d). Notably, the expression of these markers was confirmed on directly ex-vivo detected LRPAP1<sub>21–30</sub>-specific CD8<sup>+</sup> effector T cells from cohort 4 (Fig. 1d, e).

The functional capacity of LRPAP1<sub>21–30</sub>-specific CD8<sup>+</sup> T cells was assessed by their capacity to produce five different type 1 cytokines: GM-CSF, IFN $\gamma$ , TNF $\alpha$ , IL-2 and CCL4. PBMC of several patients were stimulated with LRPAP1<sub>21–30V</sub> for 10 days after which the peptide-specific cytokine production was measured by intracellular cytokine staining. Analysis revealed that LRPAP1-reactive cells mostly comprised single cytokine producers but also included T cells producing up to five different cytokines, indicating their polyfunctionality (Figure S4). Antigen-specific type 1 cytokine production was detected after vaccination in 12 out of 14 patients tested. This included one patient (O18) for which we failed to detect the response by dextramers upon TEIPP24 vaccination, thereby raising the number of vaccine responders to 20 out of 24. The

**Table 1 | Overview of baseline characteristics**

	<b>1 (20 µg)</b>	<b>2 (40 µg)</b>	<b>3 (100 µg)</b>	<b>4 (100 µg + pembrolizumab)</b>	<b>Total</b>
Number of patients	6	7	7	6	26
Median age at inclusion (range)	65 (60–70)	62 (47–69)	64 (53–79)	65 (58–69)	64 (47–79)
Gender (%)					
Male	2 (33.3)	3 (42.9)	5 (71.4)	5 (83.3)	15 (57.7)
Female	4 (66.7)	4 (57.1)	2 (28.6)	1 (16.7)	11 (42.3)
Smoking (%)					
Never	1 (16.7)				1 (3.8)
Current	3 (50.0)	2 (28.6)		3 (50.0)	17 (65.4)
Former	2 (33.3)	5 (71.4)	7 (100)	3 (50.0)	8 (30.8)
Histopathologic subtype (%)					
Adenocarcinoma	4 (66.7)	6 (85.7)	2 (28.6)	3 (50.0)	15 (57.7)
Squamous cell	2 (33.3)	1 (14.3)	5 (71.4)	1 (16.7)	9 (34.6)
Undifferentiated				2 (33.3)	2 (7.7)
Previous chemotherapy <sup>a</sup>	5 (83.3)	7 (100)	7 (100)	6 (100)	25 (96.1)
Median # of cycles [range]	4 [4–9]	8 [4–10]	4 [2–4]	4 [3–10]	4 [2–10]
Previous immunotherapy <sup>b</sup>	6 (100)	7 (100)	7 (100)	6 (100)	26 (100)
Median # of cycles [range]	5 [4–14]	8 [4–42]	7 [4–12]	12 [2–23]	7.5 [2–42]
Median time interval start TEIPP24 in weeks <sup>c</sup> [range]	10 [7–24]	10 [2–38]	11 [6–37]	10 [5–54]	11 [2–54]
Combination chemo/immunotherapy	5 (83.3)	6 (85.7)	6 (85.7)	5 (83.3)	22 (84.6)
ECOG performance status (%) <sup>d</sup>					
0	4 (66.7)		1 (14.3)	3 (50.0)	8 (30.8)
1		7 (100)	6 (85.7)	2 (33.3)	15 (57.7)
2	2 (33.3)			1 (16.7)	3 (11.5)
T- stage <sup>d</sup>					
X	2 (50.0)		1 (14.3)	2 (33.3)	5 (15.4)
0					
1	1 (16.7)	1 (14.3)	1 (14.3)	3 (50.0)	6 (23.1)
2	1 (16.7)	2 (28.6)	2 (28.6)		5 (19.2)
3		1 (14.3)			1 (3.8)
4	2 (33.3)	3 (42.9)	3 (42.9)	1 (16.7)	9 (34.6)
N- stage <sup>d</sup>					
X		1 (14.3)			1 (3.8)
0	1 (16.7)			1 (16.7)	2 (7.7)
1	1 (16.7)	1 (14.3)		1 (16.7)	3 (11.5)
2	2 (33.3)	3 (42.8)	3 (42.8)	1 (16.7)	9 (34.6)
3	2 (33.3)	2 (28.6)	4 (57.1)	3 (50.0)	11 (42.3)
M- stage <sup>d</sup>					
1a	2 (33.3)		1 (14.3)		3 (11.5)
1b		2 (28.6)	1 (14.3)		3 (11.5)
1c	4 (66.7)	5 (71.4)	5 (71.4)	6 (100)	20 (76.9)
Systemic metastases <sup>d</sup>	4 (66.7)	6 (85.7)	5 (71.4)	5 (83.3)	21 (80.8)
Location systemic metastases <sup>d</sup>					
Liver	3 (50.0)	1 (14.3)	2 (28.6)	3 (50.0)	9 (34.6)
Brain	1 (16.7)	3 (42.9)			4 (15.4)
Skeletal	4 (66.7)	3 (42.9)	3 (42.9)	2 (33.3)	11 (42.3)
Adrenal glands		2 (28.6)		4 (66.7)	6 (23.1)
Other <sup>e</sup>		1 (14.3)	1 (14.3)	2 (33.3)	4 (15.4)

ECOG Eastern Cooperative Oncology Group.

<sup>a</sup>Chemotherapy regimens consisted of carboplatin, cisplatin, pemetrexed, paclitaxel, docetaxel, gemcitabine or etoposide or a combination of any.<sup>b</sup>The immunotherapy regimen consisted of pembrolizumab, durvalumab or nivolumab.<sup>c</sup>Time interval between last immunotherapy cycle and first TEIPP24 vaccination in weeks.<sup>d</sup>At time of inclusion.<sup>e</sup>Pleural, mediastinal and axillar metastases were not included under systemic metastases.

population of cytokine producing CD8<sup>+</sup> T cells increased after each vaccination (Fig. 1f, Tables S7, S8). To show that the vaccine-expanded LRPAP1<sub>21-30</sub>-specific CD8<sup>+</sup> T cells were able to recognize TAP-impaired tumor cells, we sorted MHC dextramer positive and negative cells from the blood of three patients after vaccination and tested them against a panel of tumor cells. Vaccine-expanded LRPAP1<sub>21-30</sub>-specific CD8<sup>+</sup> T cells recognized TAP-deficient (TAPKO) 518A2 melanoma cells, but not TAP-proficient (WT) or TAP- and LRPAP1-deficient (TAPKO/LRPAP1KO) 518A2 melanoma cells (Fig. 1g and Fig. S5).

**TEIPP24 vaccination induces CD4<sup>+</sup> T cell responses in more than half of the patients**

Neoantigen vaccination reportedly induces CD4<sup>+</sup> T-cell responses to tumor-specific antigens<sup>20–24</sup>. Therefore, the immune response to the

24-mer vaccine peptide was also measured at baseline and after each vaccination in 21 patients for whom sufficient PBMC were available. PBMC were stimulated with the vaccine peptide for 10 days after which the TEIPP24 peptide-specific production of the five different cytokines was measured. In 13 out of the 21 patients tested (62%) TEIPP24-specific type 1 cytokine production by CD4<sup>+</sup> T cells was observed, of which the majority of responding CD4<sup>+</sup> T cells produced 2–5 cytokines simultaneously (Fig. S4d, e and Tables S7, S8). In general, the TEIPP24-specific T-cell response increased with each vaccination. (Fig. 2a–c). TEIPP24-specific CD4<sup>+</sup> T-cell reactivity coincided with the detection of LRPAP1<sub>21-30</sub>-dextramer-positive CD8<sup>+</sup> T cells in all 13 cases (Fig. 2a–d), while the average LRPAP1<sub>21-30</sub>-dextramer-positive CD8<sup>+</sup> T cells was also higher in this group (Fig. 2e).

**Table 2 | Overview of treatment characteristics and outcomes**

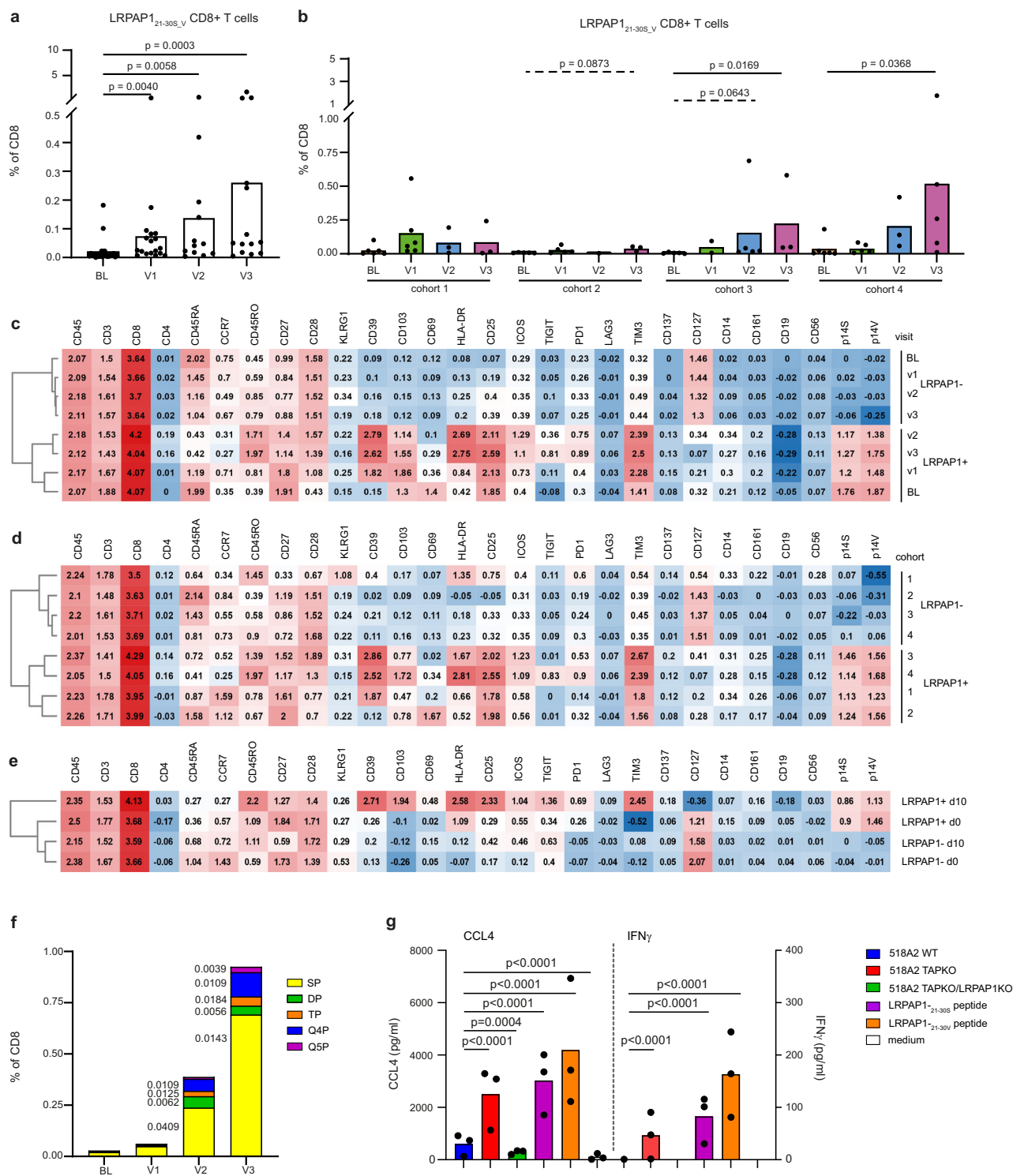
	1 (20 µg) n = 6	2 (40 µg) n = 7	3 (100 µg) n = 7	4 (100 µg + pembrolizumab) n = 6	Total n = 26
Median number of administered TEIPP24 vaccinations [range]	3 [2,3] <sup>a</sup>	3 [2,3] <sup>a</sup>	3 [2,3] <sup>a</sup>	3	3 [2,3]
Number of patients with all 3 vaccinations	5	6	6	6	23
DLT	0	0	0	0	0
SAE (patients)	3	3	2	1	9
SUSAR	0	0	0	0	0
Clinical response at week 9 <sup>b</sup>					
CR	0	0	0	0	0
PR	1	0	0	0	1
SD	2	2	1	3	8
PD	3 <sup>c</sup>	5 <sup>d</sup>	6 <sup>e</sup>	3 <sup>c</sup>	17

DLT dose limiting toxicity, OS overall survival, SAE serious adverse event, SUSAR suspected unexpected serious adverse reaction.  
<sup>a</sup>One patient received only two TEIPP24 vaccinations due to rapid clinical deterioration or radiographic progression.  
<sup>b</sup>According to RECIST 1.1 for patients that underwent radiological response evaluation according to protocol. PD progressive disease, SD stable disease, PR partial response, CR complete response.  
<sup>c</sup>For two of these patients radiological response evaluation was performed after the second TEIPP24 vaccination due to clinical deterioration. Two of these patients had mixed response.  
<sup>d</sup>For one of these patients radiologic response evaluation was performed after the first TEIPP24 vaccination due to clinical deterioration, for one patient PD was based on cerebral metastases, no new CT thorax and abdomen was performed.  
<sup>e</sup>For one of these patients radiological response evaluation was performed after the second TEIPP24 vaccination due to rapid progressive disease.

**Table 3 | Adverse events that were (possibly) related to TEIPP24 vaccination**

Adverse event <sup>a</sup>	Grade 1 n	(%)	Grade 2 n	(%)	Grade 3 n	All grades	(%)
Myalgia	4	(15.4)	0	(0.0)	0	4	(15.4)
Headache	2	(7.7)	0	(0.0)	0	2	(7.7)
Pain (contralateral) injection site	2	(7.7)	0	(0.0)	0	2	(7.7)
Xerostomia	1	(3.8)	0	(0.0)	0	1	(3.8)
Nausea	2	(7.7)	0	(0.0)	0	2	(7.7)
Malaise	2	(7.7)	2	(7.7)	0	4	(15.4)
Fever/rigors	1	(3.8)	2	(7.7)	0	3	(11.5)
Rash	1	(3.8)	0	(0.0)	0	1	(3.8)
Local skin reaction	1	(3.8)	0	(0.0)	0	1	(3.8)
Anorexia	1	(3.8)	0	(0.0)	0	1	(3.8)
Neuropathy	2	(7.7)	1	(3.8)	0	3	(11.5)
Pruritis	3	(11.5)	1	(3.8)	0	4	(15.4)
Anemia	0	(0.0)	1	(3.8)	0	1	(3.8)
Deep venous thrombosis	0	(0.0)	1	(3.8)	0	1	(3.8)
Dyspnea	1	(3.8)	1	(3.8)	0	2	(7.7)
Pain	1	(3.8)	0	(0.0)	0	1	(3.8)
Edema	1	(3.8)	0	(0.0)	0	1	(3.8)
Epistaxis	0	(0.0)	1	(3.8)	0	1	(3.8)
Total	25	(96.2)	10	(38.5)	0	35	(134.6)

Unlikely and not related adverse events are excluded.  
<sup>a</sup>All adverse events that were possibly, probably and definitely related to study medication are included in the table.



### Radiological response evaluations

In total, 24 patients had radiological response measurements. In one patient progressive disease (PD) was based on cerebral metastases without a response evaluation CT-scan (patient 11) and one patient died before response evaluation CT-scan (patient 26). Tumor response was measured in 19 patients by CT-scan three weeks after the last vaccination according to protocol. Four patients had an earlier CT-scan after two vaccinations due to clinical signs of progression (patient 3, 4, 18 and 22). In one patient a CT scan was made after the first vaccination (patient 12), because of rapid clinical deterioration.

Overall, clinical benefit (PR, SD) to single peptide vaccination (TEIPP24) according to RECIST1.1 was detected in 9 out of the 24 vaccinated patients whom were progressive on checkpoint therapy before vaccination (Table 2). The medical records of these patients confirmed progression on 2 separate CT scans before entering the trial. A total of 8 patients had stable disease (SD) after 2-3 TEIPP vaccinations (Table 2; Fig. 3a, b, Tables S9-12). The SD of patients #6, 16, 23, and 24 were confirmed. Patient 2 displayed a partial response (PR) evidenced by several shrunken lesions and the disappearance of one lesion (Fig. 3c, d). This response was confirmed in two additional scans performed at 22 and 35 weeks after the first TEIPP24



**Fig. 1 | LRPAP1<sub>21-30S</sub>-specific CD8<sup>+</sup> T-cell responses after vaccination.** The presence of circulating LRPAP1<sub>21-30</sub>-specific CD8<sup>+</sup> T cells was determined by dual LRPAP1<sub>21-30S</sub>- and LRPAP1<sub>21-30V</sub>-dextramer staining using spectral flow cytometry after one round of in vitro expansion with the LRPAP1<sub>21-30V</sub> peptide. **a, b** Percentage of LRPAP1<sub>21-30S</sub>-specific CD8<sup>+</sup> T cells in the PBMC at baseline (BL) and after 1, 2 and 3 vaccinations (v1-v3) is provided for 23 patients across **(a)** all and **(b)** the different cohorts. **c–e** Hierarchically clustered heatmaps with the protein expression levels of indicated markers on CD8<sup>+</sup> T cells non-specific (LRPAP<sup>+</sup>) or specific (LRPAP<sup>+</sup>) for LRPAP1<sub>21-30</sub>, depicted **(c)** at baseline and after 1 (V1), 2 (V2) and 3 (V3) vaccinations, **(d)** and across the different cohorts, for 20 patients with a detectable LRPAP1<sub>21-30S</sub>-specific CD8<sup>+</sup> T-cell response, and **(e)** for ex vivo (d0) and in vitro expanded (d10) CD8<sup>+</sup> T cells after 3 vaccinations ( $n = 2$  patients from cohort 4). Marker expression is shown as z-score of median signal intensity per channel. Blue: low expression, red: high expression. **f** Percentage of single (SP; yellow), double (DP; green), triple (TP; orange), quadruple (Q4P; blue), and quintuple (Q5P; purple) cytokine-positive LRPAP1<sub>21-30V</sub>-specific CD8<sup>+</sup> T cells is depicted at baseline (BL) and after 1, 2 and 3 vaccinations (v1-v3) with the TEIPP24 vaccine for 13 patients in which we could

purple) cytokine-positive LRPAP1<sub>21-30V</sub>-specific CD8<sup>+</sup> T cells is depicted at baseline (BL) and after 1, 2 and 3 vaccinations (v1-v3) for 12 patients in which we could detect LRPAP1<sub>21-30S</sub>-specific CD8<sup>+</sup> T cells by dual dextramer analysis and had sufficient cells to perform additional intracellular cytokine staining. P-values versus baseline are indicated at the side of the bar. **g** LRPAP1<sub>21-30S</sub>-specific CD8<sup>+</sup> T cells were isolated from three patients after vaccination by dextramer-guided flow sorting, after which the LRPAP1 dextramer-positive T cell fractions were expanded and tested against WT, TAPKO and TAPKO/LRPAP1KO 518A2 melanoma cells (blue, red and green, respectively) as well as the LRPAP1<sub>21-30S</sub> and <sub>21-30V</sub> peptides (purple and orange, respectively). CCL4 (left) and IFN $\gamma$  (right) production is determined by ELISA after overnight co-incubation of the T cells with the target cells. Data are represented as scatter plots with bars indicating mean and dots representing individual data points (**a, b, g**) or as stacked bars (**f**). Statistical analysis by unpaired non-parametric Kruskal-Wallis with Dunn's multiple comparisons test (**a, b, f, g**). Source data are provided as a Source Data file.

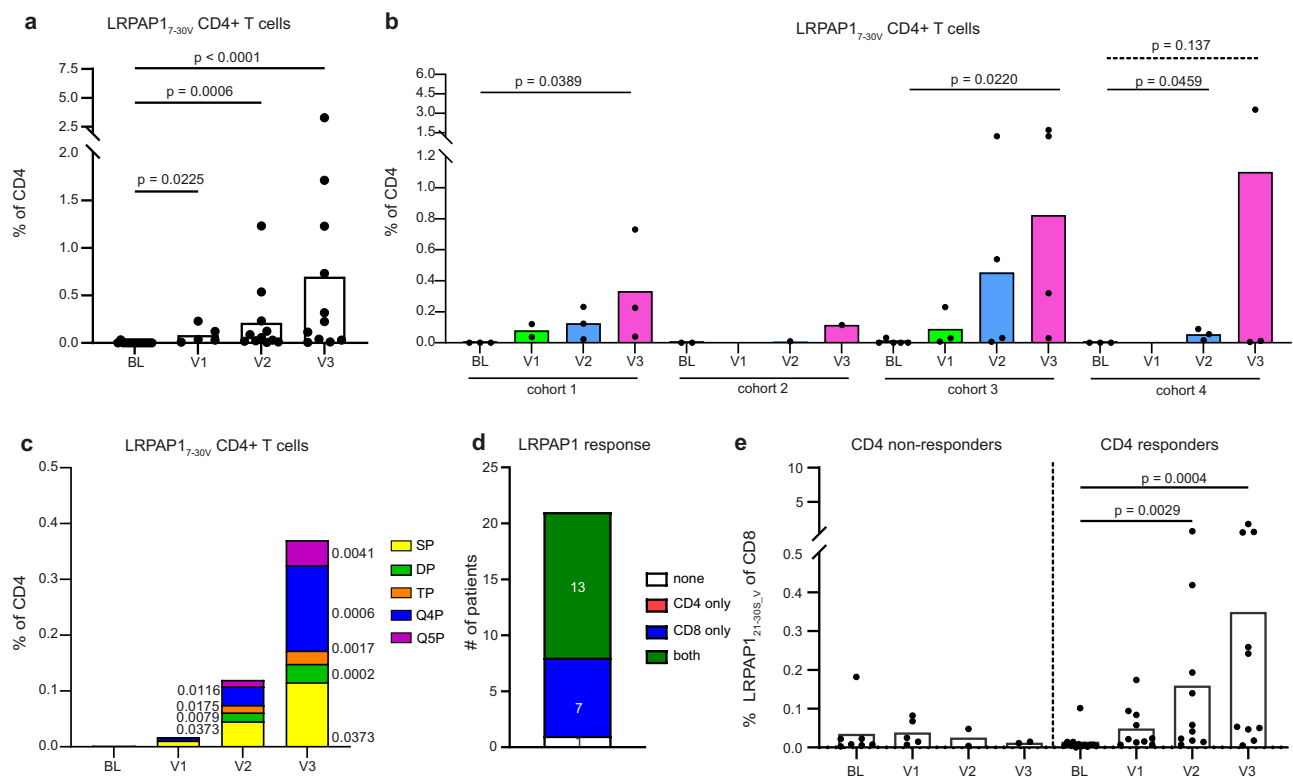


**Fig. 2 | The presence of circulating LRPAP1<sub>7-30V</sub>-specific CD4<sup>+</sup> T cells after one round of in vitro expansion with the TEIPP24 peptide.** TEIPP24 peptide-expanded cells were stimulated with non-loaded (medium) or TEIPP24-peptide-loaded autologous monocytes in the presence of brefeldin A. Subsequently, the cells were stained with antibodies against CD3, CD4, CD8, CD137, CD154, GM-CSF, IFN $\gamma$ , TNF $\alpha$ , IL2 and CCL4. Cells were gated as described in fig. S4. **a, b** Percentage of LRPAP1<sub>7-30V</sub>-specific CD4<sup>+</sup> T cells in the PBMC at baseline (BL) and after 1, 2 and 3 vaccinations (V1-V3) is provided for 13 patients in which we could detect LRPAP1<sub>7-30V</sub>-specific CD4<sup>+</sup> T cells across **(a)** all and **(b)** the different cohorts. **c** Percentage of single (SP; yellow), double (DP; green), triple (TP; orange), quadruple (Q4P; blue), and quintuple (Q5P; purple) cytokine-positive LRPAP1<sub>7-30V</sub>-specific CD4<sup>+</sup> T cells is depicted at baseline (BL) and after 1, 2 and 3 vaccinations (v1-v3) with the TEIPP24 vaccine for 13 patients in which we could

detect LRPAP1<sub>7-30V</sub>-specific CD4<sup>+</sup> T cells. P-values versus baseline are indicated at the side of the bar. **d** Number of patients displaying either no (none; white), only a CD4<sup>+</sup> T cell (red), only a CD8<sup>+</sup> T cell (blue), or a combined (both) CD4<sup>+</sup> and CD8<sup>+</sup> T-cell response (green) after vaccination. **e** Percentage of LRPAP1<sub>21-30S</sub>-specific CD8<sup>+</sup> T cells in the PBMC of the 21 patients tested for the reactivity of both CD4 and CD8 T cells, at baseline (BL) and after 1, 2 and 3 vaccinations (v1-v3) for patients without and with a detectable LRPAP1-specific CD4<sup>+</sup> T-cell response (CD4 non-responders (left) and CD4 responders (right)). Data are represented as scatter plots with bars indicating mean and dots representing individual data points (**a, b, e**) or as stacked bars (**c, d**). Statistical analysis by unpaired non-parametric Kruskal-Wallis with Dunn's multiple comparisons test (**a, b, c, e**). Source data are provided as a Source Data file.

vaccination. Interestingly, in patient 3 with PD, the radiographic evaluation showed decrease in size of the target lesions, mainly of the primary tumor. In addition, patient 22 showed progression based on non-target lesions during the CT-scan after vaccination 2 but showed a mixed response during a follow-up scan, 10 weeks after completing the treatment scheme. The sum of the target lesions decreased by 14%. This suggests a mixed response (MR) of the tumors in these two patients, indicative that some of their

tumors were sensitive to TEIPP vaccination. Therefore, a total of 11 PR, SD and MR were observed in 24 radiologically evaluable patients. There were no indications that clinical parameters, including the number of cycles or type of chemotherapy, the time interval between last checkpoint therapy and start of TEIPP24 vaccination, or secondary resistance checkpoint blockade (defined as at least 12 weeks checkpoint blockade before vaccination<sup>25</sup>) influenced clinical outcome.

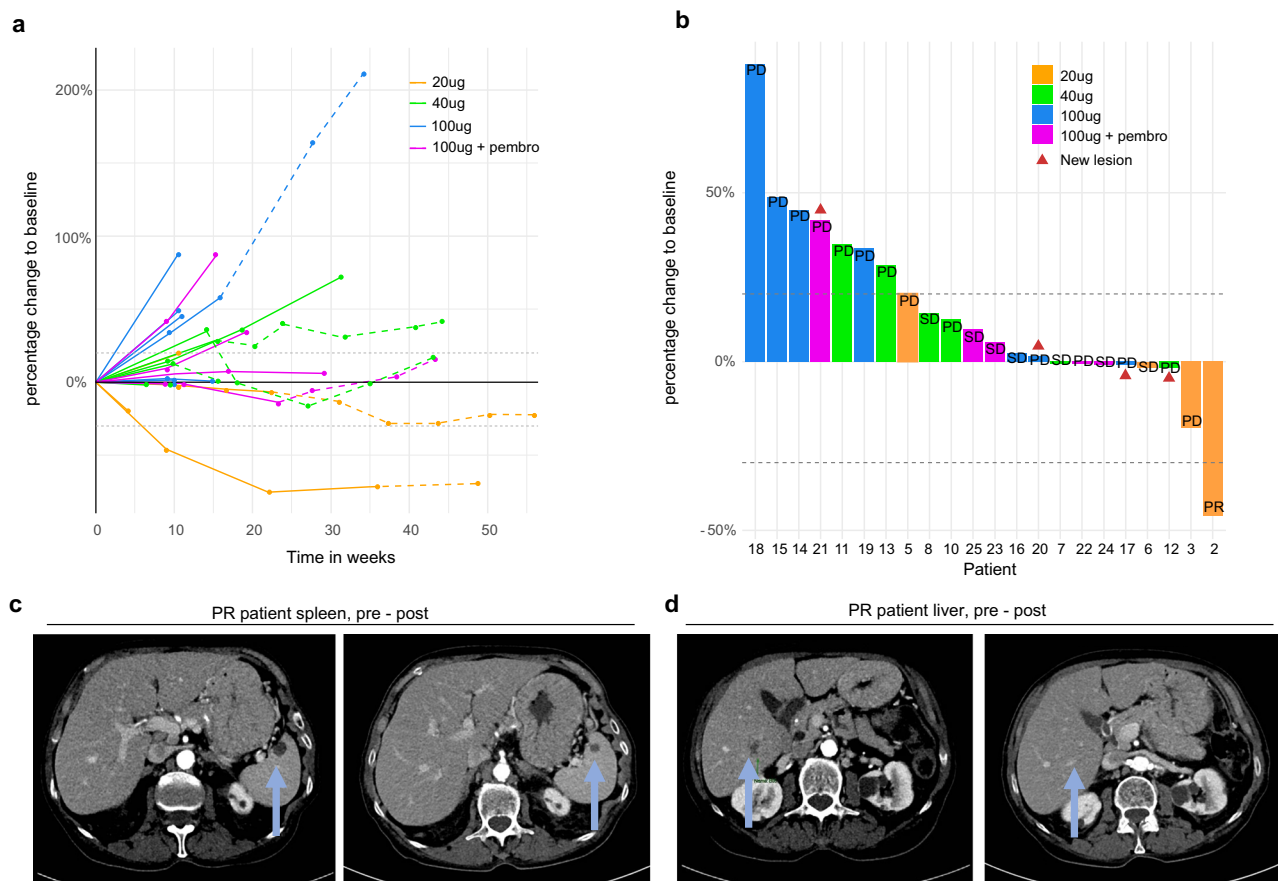


**Fig. 3 | Radiological responses of TEIPP24 vaccinated patients. a** Spider plot depicting the percentage change of the sum of target lesions compared to the baseline measurement. The dashed line indicates the start of a new treatment. Data given for 22 patients with baseline target lesions and follow-up measurements. **b** Waterfall plot with the best percentage change in the sum of the target lesions per patient for 22 patients with baseline target lesions and follow-up measurements.

The response of the patient at week 9 is depicted in the end of the bar. The different colors in (a, b) indicate the different treatment cohorts of 20  $\mu$ g (orange), 40  $\mu$ g (green), 100  $\mu$ g (blue) peptide and 100  $\mu$ g peptide + pembrolizumab (purple). **c, d** CT-scan of patient 2 where the change of two target lesions is indicated by the light blue arrow. Source data are provided as a Source Data file.

### Follow-up and relation to vaccine-induced T cell reactivity

Follow-up data for PFS and OS were obtained up to October 29nd 2024. A total of seven patients completed the 52 week follow-up, they all received a third or fourth (#13,#21) line treatment (non-immunotherapy) after progression on TEIPP24 vaccination. Figure 4a shows a swimmer's plot of all included patients. The median follow-up for surviving patients was 8.3 months. A total of 25 out of the 26 patients had progression after TEIPP24 vaccination during this follow-up. Interestingly, patient 24 still displays clinical benefit after the combination of TEIPP24 vaccination and pembrolizumab and subsequent continuation on checkpoint blockade. A trend towards prolonged OS ( $p=0.12$ ) was observed for patients displaying clinical benefit compared to the group without clinical benefit after vaccination (Fig. 4b). Median PFS was 2.1 months (IQR 1.8–4.2 months) (Fig. 4c). Stratification per cohort resulted in a median PFS of 2.0 months (IQR 1.3–5.4) for cohort 1, 2.1 months (IQR 1.8–2.1) for cohort 2, 2.1 months (IQR 2.0–2.1) for cohort 3, and 3.5 months (IQR 1.4–9.6) for cohort 4. A total number of 14 patients received follow-up treatment, while 18 patients deceased during follow-up, resulting in a median OS of 9.4 months (IQR 4.0–14.7) (Fig. 4d). Comparison of the vaccine-induced CD8<sup>+</sup> T-cell response in patients with ( $n=11$ ) or without ( $n=13$ ) PR, SD or MR, revealed that the group of patients with such a response displayed on average a stronger LRPAP1<sub>21-30</sub>-specific CD8<sup>+</sup> T-cell response (Fig. 4e).

### Potential blood biomarkers for therapy success or failure

We analyzed the immune phenotypes of PBMC, available for 20 patients, in order to determine potential predictive biomarkers to therapy response. A 29 parameter spectral flow cytometry panel (Table S13) in combination with the cloud-based OMIQ data analysis software<sup>26</sup> was used to visualize and quantify the several different circulating immune cell populations before therapy, and a total of 31 different populations were identified (Fig. 5a, Fig. S6, Table S14). The frequencies of these populations differed per patient but generally were not altered during therapy (Fig. S7).

To reveal a potential association with vaccine responsiveness, patients were divided according to the strength of their LRPAP1<sub>21-30</sub>-specific CD8<sup>+</sup> T-cell response or of their CD4<sup>+</sup> TEIPP24-specific T-cell response (Fig. 5b–i, Fig. S8). The frequency of populations 3 (CD8<sup>+</sup> central memory T cells, Tcm), 5 (CD8<sup>+</sup> naïve T cells, Tn), 7 (CD4<sup>+</sup> Tn), 11 (CD4 and CD8 double negative, DN Tn) and 22 (CD4<sup>+</sup> KLRG1<sup>+</sup> Tcm), were higher in patients displaying a relative higher LRPAP1<sub>21-30</sub>-specific CD8<sup>+</sup> T-cell response. A higher frequency of population 5 was also associated with a stronger CD4<sup>+</sup> T-cell response (Fig. 5c). In contrast, populations 18A (monocytes) and 18B (monocytic MDSC, mMDSC) or together (“total monocytes”) were associated with a relative lower response, both of CD4<sup>+</sup> and CD8<sup>+</sup> T cells (Fig. 5g–i). The negative effect of these monocytic populations on vaccine-induced T-cell responses confirm other reports<sup>16,27</sup>. In addition, the patients were divided into two cohorts.

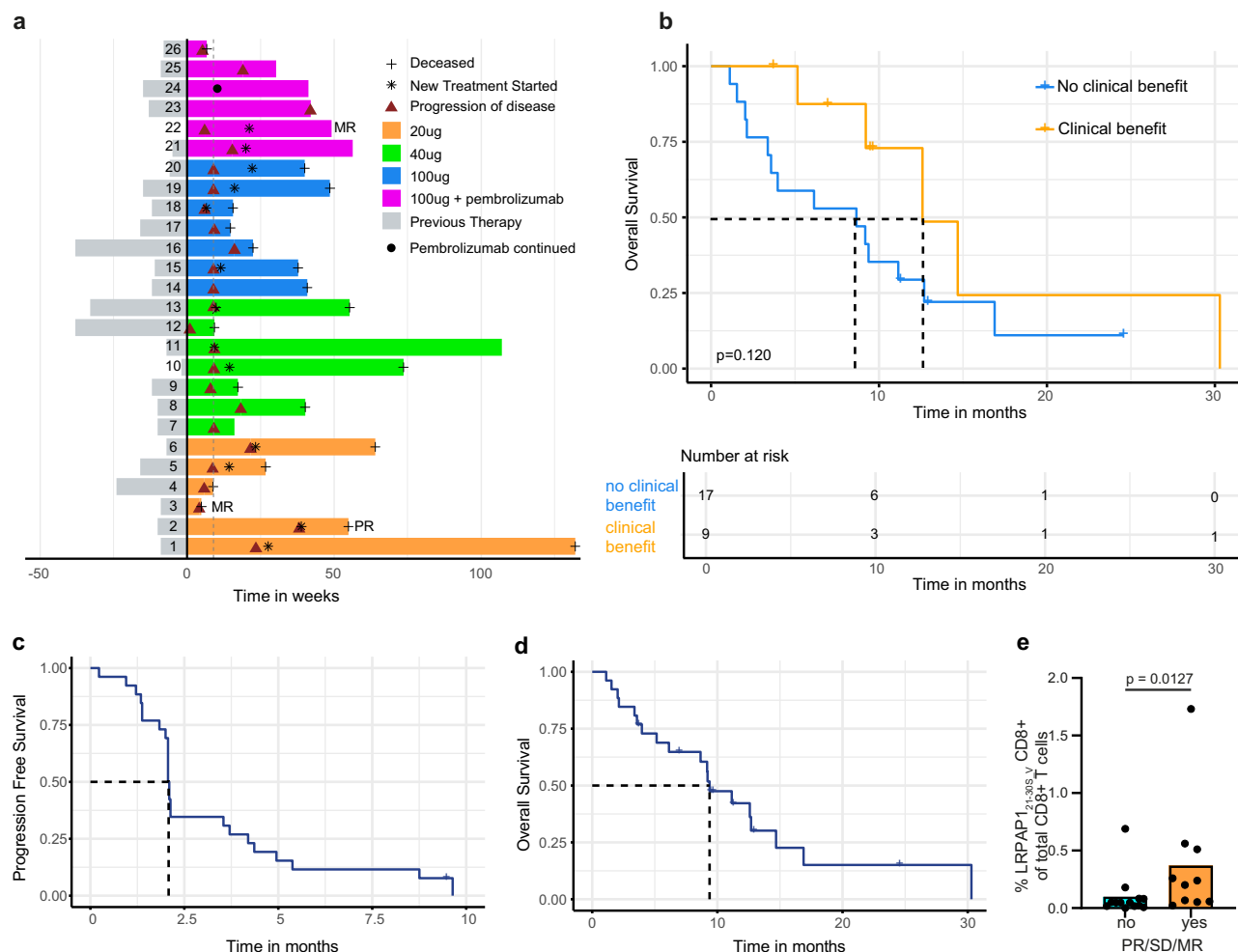


**Fig. 4 | Clinical benefit in relation to vaccine-induced immunity.** **a** Swimmer plot of the 26 patients indicating the progression free survival and overall survival. Data is given per cohort (20 µg (orange), 40 µg (green), 100 µg (blue) peptide and 100 µg peptide + pembrolizumab (purple)). The patients with PR and MR are indicated. The duration of SD reaches from the assessment at week 9 until the symbol indicating PD. The SD of patients #6, 16, 23, and 24 were confirmed. Symbols indicate: plus sign: deceased, asterisk: new treatment started, red triangle: progression of disease, black square: pembrolizumab continued. **c, d** Kaplan-Meier curves showing **(b)** the overall survival of 26 patients with (orange; median 12.69 (CI = 9.21-

undefined) months) and without (light blue; median 8.6 (CI = 3.57-undefined) months) clinical benefit after vaccination, and **(c)** progression free (median 2.08, CI = 2.07-4.20 months) and **(d)** overall survival (median 9.37 (CI = 6.13-16.89) months) of the entire patient cohort. **e** Percentage of vaccine-induced LRPAP1<sub>21-30</sub>-specific CD8<sup>+</sup> T cells in patients with (yes; orange) or without (no; light blue) a PR, SD or MR after vaccination. Data is represented as scatter plot with bars indicating mean and dots representing individual data points. Statistical analysis **(b, c, d)** by non-parametric log rank tests and **(e)** two-tailed, unpaired non-parametric Mann-Whitney U test. Source data are provided as a Source Data file.

The group of PR, SD, and MR versus the group of patients with PD after therapy but no differences were found in the frequencies of populations (Fig. S9).

## Discussion

This first-in-human TEIPP study shows that the administration of TEIPP24 vaccine, at different dosages and in combination with pembrolizumab, does not result in dose limiting toxicity in patients with advanced NSCLC progressive on checkpoint blockade. The vaccine induced a LRPAP1<sub>21-30</sub>-specific CD8<sup>+</sup> T-cell response in more than 80% of the patients and this exceeds the preset success value of 30% at this phase. The magnitude, activation status and polyfunctionality of the LRPAP1<sub>21-30</sub>-specific CD8<sup>+</sup> T-cell response was influenced by the vaccine dose, number of vaccinations administered, the induction of a vaccine-specific CD4<sup>+</sup> T-cell response and the presence of mMDSC in the circulation before start of treatment. In general, the LRPAP1<sub>21-30</sub>-specific CD8<sup>+</sup> T-cell response was best developed after three vaccinations. This is in line with a recent in-depth study using T cell epitope SLP vaccines in mice, indicating that the differentiation of the vaccine-elicited CD8<sup>+</sup> T cells depends on repeated vaccination and that a third

vaccination specifically augments effector-memory and tissue-resident memory CD8<sup>+</sup> T-cell formation, as evidenced by activation-associated cell-surface markers and their polyfunctional cytokine production<sup>28</sup>. Repeated vaccination with at least seven prime and booster injections has been used for mutation-specific neoantigen vaccines and resulted in strong ex-vivo detectable responses<sup>23,29,30</sup>, suggesting that stronger vaccine induced LRPAP1<sub>21-30</sub>-specific CD8<sup>+</sup> T-cell responses may be achieved when the number of injections is increased. Minimal LRPAP1<sub>21-30</sub>-specific responses were detected pre-vaccination, consistent with the notion that their priming is likely to be a rare event as TEIPP are presented at the cell surface only by cells with defects in antigen presentation<sup>31</sup>.

Together our study provides several key findings. First, the vaccination activated TEIPP-specific T cells in the absence of high grade adverse events. The observations of one PR, eight SDs and two MRs in patients progressive on first line treatment, suggest some form of vaccine-induced T-cell mediated tumor control, albeit limited. A number of patients were recruited into the trial shortly after being diagnosed with progression after first line ICB, posing the question if the clinical effect observed after vaccination may reflect a



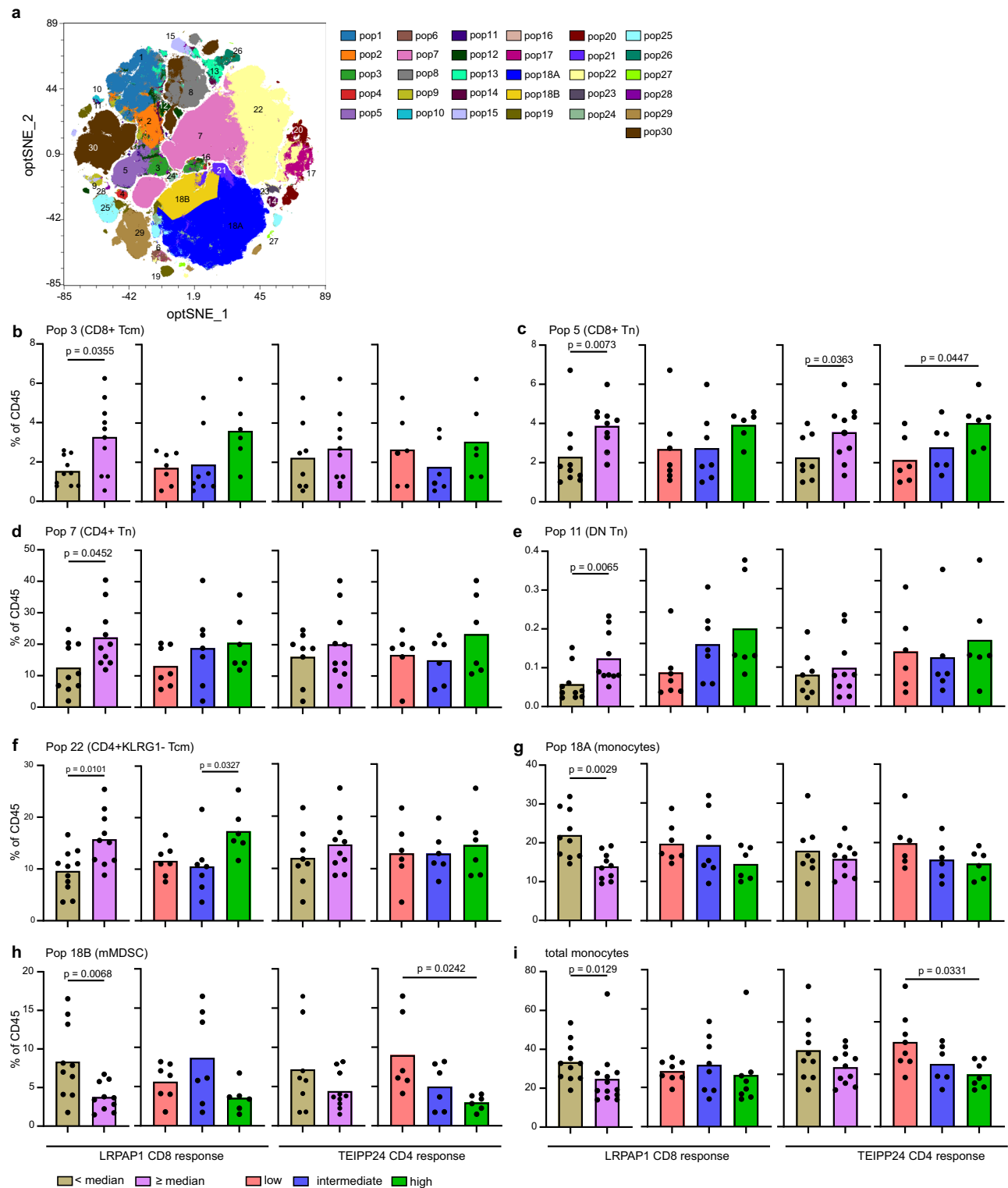


**Fig. 5** | PBMC collected at baseline, and after 1, 2 and 3 vaccinations from 20 patients for which we had sufficient cells to perform ex vivo analysis were stained with a combined immunophenotyping/dextramer panel of 29 markers (see supplementary table II). High-dimensional single cell data analysis of the stained PBMC were performed by opt-distributed Stochastic Neighbor Embedding (optSNE) and FLOW SOM using OMIQ. **a** optSNE plot visualizing cluster partitions by FLOW SOM for all patient samples. **b–i** Frequencies of populations 3 (pop3 CD8<sup>+</sup> Tcm (**b**)) pop5 (CD8<sup>+</sup> Tn, (**c**)) pop7 (CD4<sup>+</sup> Tn, (**d**)) pop11 (DN Tn, (**e**)) pop22 (CD4<sup>+</sup> KLRG1<sup>+</sup> Tcm, (**f**)) pop18A (monocytes, (**g**)) pop 18B (mMDSC, (**h**)) and total monocytes (**i**) at baseline is shown as percentage of CD45<sup>+</sup> cells for patients in

relation to the strength of the LRPAP1<sub>21-30S</sub>-specific CD8<sup>+</sup> T-cell response (left two panels) or LRPAP1<sub>7-30V</sub>-specific (TEIPP24) CD4<sup>+</sup> T-cell response (right two panels), respectively. Patients were grouped into low or high T-cell responses based on the median response (i.e. <median (gold) and > median (purple)) or based on tertiles (i.e. lowest 33% (low; red), middle 33% (intermediate; blue) or highest 33% (high; green)). Data are represented as scatter plots with bars indicating mean and dots representing individual data points (**b–i**). Statistical analysis by two-tailed, unpaired non-parametric Mann-Whitney U test (2 groups) or unpaired non-parametric Kruskal-Wallis with Dunn's multiple comparisons test (3 groups). Source data are provided as a Source Data file.

phenomenon called pseudoprogression<sup>32</sup>. It is, however, challenging to distinguish true disease progression from pseudoprogression and there currently is no reliable method to assess this<sup>32</sup>. In two cases with clinical benefit after vaccination, ICB was stopped early after the standard 4 cycles, and one of these cases started vaccination 1 month afterwards. Two other patients started vaccination within 2 months after stopping ICB but had received 11 and 12 cycles of ICB. Importantly, all patients with clinical benefit were diagnosed with progression on at least 2 separate CT scans before entering the trial. While we can't completely exclude pseudoprogression for the one patient with disease progression within the first 12 weeks of ICB and vaccinated rapidly afterwards, pseudoprogression is deemed unlikely for the other patients. Clinical outcome was also not related to other clinical parameters, the interval to last checkpoint therapy, secondary resistance to checkpoint blockade<sup>25</sup>, the inflammatory state of the tumor or tumor-expressed PD-L1, but it was associated with a stronger vaccine-induced LRPAP1<sub>21-30</sub>-specific CD8<sup>+</sup> T-cell response. The observation of T cell related clinical benefit, in the absence of major adverse events, validates the applicability of this new class of ubiquitous, nonmutated and immunogenic self-antigens as targets for immunotherapeutic approaches. This is in agreement with our extensive studies in murine cancer models<sup>11-13</sup>.

Second, our observations suggest that although TEIPP24 may be active as a single agent in cohorts 1-3, it also synergizes with anti-PD1 therapy in patients progressive on earlier PD-1 blockade. In the two cohorts receiving the highest dose (100 µg) of the vaccine, the LRPAP1<sub>21-30</sub>-specific CD8<sup>+</sup> T cells expressed PD-1. Co-treatment with anti-PD1 in cohort 4 resulted in the expansion of LRPAP1<sub>21-30</sub>-specific CD8<sup>+</sup> T cells to a level that they could be detected directly ex-vivo. PD-1 restrains the expansion of antigen-specific T cells at priming or boosting<sup>33,34</sup>, most likely this occurs at the level of the peripheral dendritic cell dependent T-cell activation<sup>35-37</sup>. We, therefore, chose to provide pembrolizumab at each vaccination of the patients in cohort 4. In line with our results, PD-1 blockade has been shown to result in the expansion of tumor-specific T cells in the blood<sup>38</sup>. One patient in cohort 4 is still without progression and continued to be treated with checkpoint blockade after initial response to TEIPP24 vaccination. Regained sensitivity to PD-1 blockade has also been observed with melanoma FixVac treatment after PD-1 blockade failure<sup>24</sup>.

Third, this first-in-human TEIPP vaccine comprised a single CD8<sup>+</sup> T cell epitope only, as this study was entertained to function as a proof of concept for the safety and immunogenicity of this new class of cancer antigens that TEIPP is in humans. Earlier trials revealed that the strength of the vaccine-induced anti-tumor response, defined by the breadth and magnitude of the T-cell response to multiple epitopes, is associated with a more prominent clinical outcome to a multiple SLP therapeutic HPV16 vaccine in high grade pre-cancers<sup>15,39</sup> and cervical cancer<sup>16</sup>. Similarly, tumors were successfully targeted with vaccines containing up to 20 neoantigens<sup>23,29,30,40</sup>. Hence, TEIPP vaccination is expected to improve on the limited clinical benefit already observed, when several TEIPP epitopes are combined into one vaccine. Our observation that the strength of the LRPAP1<sub>21-30</sub>-specific CD8<sup>+</sup> T-cell response was positively related to co-induction of a vaccine-specific CD4<sup>+</sup> T-cell response and negatively associated with the pre-treatment presence of mMDSC, reiterates the results of earlier studies showing the requirement of CD4<sup>+</sup> T-cell epitopes to boost the response of CD8<sup>+</sup> T cells during vaccination<sup>41</sup> and those demonstrating the negative impact of mMDSC on response induction by therapeutic vaccines<sup>16,27</sup>.

Clearly, our study has a number of limitations. As measurable disease according to RECIST 1.1 was not an inclusion criterion, two patients had no measurable disease at baseline. For these patients radiological response evaluation was based on non-target disease which cannot be easily quantified. In addition, while the study protocol only included radiological response evaluations at week 9 and 52, the

patients were scanned every 3 months in accordance with Dutch guidelines if possible. Unfortunately, no reliable statements on PFS could be made for patients with SD after three TEIPP24 vaccinations, due to absence of a standardized follow-up scheme. Therefore, radiological response of some patients is based on scans from other hospitals where patients may have received a 3rd line treatment, and only descriptive results could be presented. In addition, no radiologic assessment of the brain was performed. Our data included two patients who developed symptomatic brain metastases before the third vaccination whereafter radiologic imaging was done. It remains unknown whether these metastases were present before the start of the study. Finally, at this stage of TEIPP vaccine development the downregulation of TAP in the patient's tumor was not an inclusion criterium. The absence of TAP downregulation may prevent the tumor to respond to the vaccine.

The positive outcome of this first-in-human single TEIPP epitope phase I/II vaccination study provides a solid basis to move forward the concept of TEIPP targeting for tumor therapy. Improvements are likely to come from an increase in the number of vaccinations, the addition of more TEIPP epitopes to the vaccine as well as cotreatment with PD-1 blockade. Since many different tumors display TAP downregulation at a high frequency<sup>3-8</sup>, TEIPP targeting modalities are considered to be widely applicable.

## Methods

### Study design and ethics statement

This first-in-human multi-center, open label, non-randomized, phase I/II dose escalation study with extension cohort utilized the standard 3 + 3 design for phase I trials that was adapted according to earlier recommendations for proof-of-principle vaccine trials to have a cohort size of at least 6 patients per cohort, and a minimum of 20 patients in the investigated population<sup>42</sup>. The trial was conducted in the Erasmus Medical Center (EMC) Cancer Institute in Rotterdam and the Leiden University Medical Center (LUMC) in Leiden, the Netherlands. HLA-A\*02:01 positive NSCLC patients were enrolled in three cohorts of six patients (20, 40, 100 µg of peptide) with one extension cohort of six patients at the highest safest dose combined with a PD-1 checkpoint inhibitor (pembrolizumab). Patients were sequentially enrolled by assessing the safety after three out of six patients at the previous dose level had completed vaccine therapy. Patients who had not received at least two vaccinations with TEIPP24 and for whom no pre-vaccination blood sample and two post-second vaccination blood samples have been collected (all with sufficient peripheral blood mononuclear cells; PBMCs) were not evaluable for the HLA-A\*02:01-restricted LRPAP1<sub>21-30</sub>-specific CD8<sup>+</sup> T-cell assays and could be replaced unless treatment was stopped prematurely due to toxicity. This trial was conducted in accordance with the Declaration of Helsinki and good clinical practice guidelines following approval by the central committee on research involving human subjects (CCMO; NL75654.000.20) and the medical ethical committee Erasmus MC (MEC 2021-0456) and the institutional review board of Leiden University MC (L22.051). All patients provided written informed consent. The first patient was recruited on 29-09-2021, the last patient on 11-03-2024. The last follow-up point for PFS and OS was 29-10-2024.

### Eligibility criteria

Eligible patients were ≥18 years in age, with an expected life expectancy of at least 3 months, and diagnosed with HLA-A\*02:01-positive advanced NSCLC (EudraCT 2020-005427-36; NL75654.000.20; NCT05898763). Patients were eligible if they failed first-line therapy of checkpoint blockade with or without chemotherapy (i.e. progression after minimally four cycles) and couldn't endure or were not willing to receive second line treatment with docetaxel chemotherapy. Diagnosis of advanced NSCLC had to be pathologically and radiologically confirmed. HLA-A\*02:01 positivity was confirmed by high resolution

next generation sequencing (NGS) at the HLA typing laboratory of LUMC (accredited by the European Federation for Immunogenetics and for ISO15189). Only HLA-A\*0201 positive patients were included. Other factors required for inclusion were: Eastern Cooperative Oncology Group (ECOG) performance status of 0–2 and adequate renal and hepatic function as defined by creatinine clearance > 40 mL/min based on the Cockcroft-Gault glomerular filtration rate (GFR), serum total bilirubin  $\leq 2.5 \times$  upper limit of normal (ULN) unless considered due to hepatic metastases and aspartate aminotransferase (AST), alanine aminotransferase (ALT), and alkaline phosphatase (ALP)  $\leq 3.0 \times$  ULN, unless considered due to hepatic metastases.

### TEIPP24 vaccine

The TEIPP24 vaccine is an off the shelf synthetic long peptide vaccine, which is dissolved in dimethylsulfoxide, diluted with water for injection (WFI) and emulsified with Montanide ISA-51 (Seppic).

### Study procedures, outcomes and assessments

An overview of the study procedures is provided by Fig. S1. If patients were potential eligible to participate based on histological confirmed NSCLC and progressive on first line therapy, pre-screening was performed by HLA typing. If a patient was HLA-A\*0201 positive, additional screening procedures concerning standardized blood tests and a physical examination were done. The TEIPP24 vaccine was administered three times with an interval of three weeks via one subcutaneous (SC) injection in an alternating limb. Study protocol demanded a CT-scan performed at 9 weeks and at 52 weeks. Additional CT scans made during standard of care were used to further analyze radiological response.

The primary objective of the study was to determine the safety and tolerability, as well as the immunogenicity (defined as an increase in HLA-A\*0201-restricted LRPAP21-30-specific CD8<sup>+</sup> T-cells) of the TEIPP24 vaccine at different doses. Toxicity was scored according to NCI-CTCAE version 5.0. All serious adverse events (SAEs) and suspected unexpected serious adverse reactions (SUSARs) that occurred during active treatment were monitored and reported. Secondary objectives were to assess the specificity and immune modulatory effects of the vaccine, to study antigen and immune status of the patients, to determine progression free (PFS) and overall survival (OS), as well as determine the radiological tumor response and its duration up to one year after first vaccination according to RECIST v.1.1 criteria. PFS was defined as the time interval between the first TEIPP24 vaccination and date of progression of disease (radiographic or clinical progression) or date of last follow-up visit in censored cases. OS was defined as the time interval between the first TEIPP24 vaccination and date of death or date of last follow-up visit in censored cases.

### Immune monitoring

**Peripheral blood mononuclear cells.** Heparinized venous blood was collected for immunological monitoring at several time points before and during TEIPP24 vaccination and processed within 6 hours. Peripheral blood mononuclear cells (PBMC) were isolated using Ficoll density centrifugation and stored in the liquid nitrogen until use.

**TEIPP T-cell culture and reactivity testing.** TEIPP24-specific immunity was determined by measuring HLA-A\*0201-restricted LRPAP1<sub>21-30</sub>-specific CD8<sup>+</sup> T-cell reactivity and LRPAP1<sub>7-30V</sub>-specific CD4<sup>+</sup> T-cell reactivity in the blood before and after TEIPP24 vaccination. For the detection of LRPAP1-specific CD8<sup>+</sup> T-cell recognition, cryopreserved PBMCs were thawed, 2–3 million cells were directly used for MHC dextramer staining and the remaining (3–5 million) cells incubated for 2 h with 2.5 µg/mL LRPAP1<sub>21-30V</sub> peptide at 37 °C and 5%CO<sub>2</sub>, centrifuged and cultured in X-vivo 15 medium (Lonza) supplemented with 10% human AB serum (ZenBio) and 20 IU/mL recombinant human IL-2 (Aldesleukin). On days 2, 4 and 7 half of the medium was replenished with culture medium and rhIL-2 (final concentration 20 IU/mL). On day

10, the in vitro expanded PBMC were tested for the presence of LRPAP1<sub>21-30</sub>-specific CD8<sup>+</sup> T cells by MHC dextramer staining and/or intracellular cytokine staining (ICS). For the latter, the cells were restimulated overnight with medium or 10 µg/mL LRPAP1<sub>21-30V</sub> peptide. For the detection of TEIPP24-specific CD4<sup>+</sup> T cells, PBMC cultures were cultured as above, but with 2.5 µg/mL of the long LRPAP1<sub>7-30V</sub> peptide. At day 10, in vitro expanded PBMC were restimulated overnight with non-loaded and TEIPP24 peptide loaded autologous monocytes, and reactivity was determined by ICS.

**T-cell reactivity assays.** For MHC dextramer staining the cells were first incubated for 20 minutes at room temperature (RT) in the dark with Live/Dead stain, after which the cells were washed and subsequently incubated for 10 min at RT in the dark with PBS/50% fetal calf serum (FCS, Serana). Next, the cells were incubated with HLA-A\*0201 control dextramers or, LRPAP1<sub>21-30S</sub> and LRPAP1<sub>21-30V</sub> or FluMI<sub>58-66</sub> (GILGFVFTL) and CMV pp65<sub>495-503</sub> (NLVPMVATV; all from Immudex) in PBS/5% FCS/d-Biotin (Avidity) for 10 min at RT in the dark, after which the cells were washed and incubated with 50 µL PBS/0.5%BSA containing 2.5 µL human TruStain FcX blocking solution (Biolegend) for 10 minutes on ice to block Fc receptors. Next, cells were stained with cell surface markers (Tables S13a, S13b) for 30 min at RT in the dark. Finally, the cells were washed twice and resuspended in PBS/5% FCS. Acquisition of the samples was done within 2 hours on a BD LSR Fortessa using Diva 8.02 acquisition software or a 5 laser Aurora (Cytek) spectral analyzer using SpectroFlo acquisition software version 3.2.1 at the Flow core facility of the LUMC. Dextramer+ cells were identified by manual gating using FlowJo software V10.8.1. Cells were gated for singlets, live, CD45<sup>+</sup>, CD14<sup>+</sup>, CD19<sup>+</sup>, CD3<sup>+</sup> and CD8<sup>+</sup>. Gates for dextramer-positivity were set on the negative control dextramers. A response is considered antigen-specific when the percentage exceeds two times the control dextramers and has at least 10 positive spots in the gate. A gating example for this sequential gating is depicted in Figure S2.

ICS was performed following overnight incubation of T cells with medium or target peptide (as above) in the presence of 10 µg/mL Brefeldin A. Staining was performed with antibodies as listed in supplemental Table 8. In brief, cells were harvested and washed with ice-cold PBS, fixed with 50 µL of 4% paraformaldehyde on ice for 4 min, after which the cells were permeabilized by PBS/0.5%BSA/0.1% saponin and stained for 30 min on ice. Acquisition was done on an LSR II Fortessa (BD biosciences). Specific cytokine-producing T cells were identified by manual gating using FlowJo software V10.8.1. Cells were gated for live, single cells, CD3, CD4 and CD8 expression. Activated CD4<sup>+</sup> and CD8<sup>+</sup> cells were selected based on CD137 and/or CD154 expression and further analyzed for IFN $\gamma$ , TNF $\alpha$ , GM-CSF, IL2 and CCL4 expression. To this end, cells were first gated for IFN $\gamma$  and GM-CSF, yielding IFN $\gamma$ <sup>+</sup> GM-CSF<sup>+</sup>, IFN $\gamma$ <sup>+</sup> GM-CSF<sup>+</sup>, IFN $\gamma$  GM-CSF<sup>+</sup> and IFN $\gamma$  GM-CSF<sup>+</sup> populations. Next, these four populations were gated for TNF $\alpha$  and IL2 (i.e., TNF $\alpha$ <sup>+</sup> IL2<sup>+</sup>, TNF $\alpha$ <sup>+</sup> IL2<sup>+</sup>, TNF $\alpha$  IL2<sup>+</sup> and TNF $\alpha$  IL2<sup>+</sup> populations), followed by subsequent gating on CD4 or CD8 and CCL4. Cytokine gates were set on total CD4<sup>+</sup> and CD8<sup>+</sup> T cells (reference plots). A gating example for this sequential gating is depicted in Fig. S4. All possible cytokine combinations are given in Table S7. A positive response was defined as at least two times the value of the negative control, and at least 10 positive spots in the gate for any of the 5 cytokines analyzed. The total frequency of LRPAP1-reactive T cells is calculated as the SUM of all possible cytokine combinations as depicted in Table S7.

**Immunophenotyping of PBMC.** Immunophenotyping of ex vivo PBMC samples was performed for 20 patients that were stained with the 29 marker panel (including LRPAP1-dextramers; as above) and acquired on the 5 laser Aurora. Testing of unmixing accuracy was done using FlowJo software. High-dimensional single cell data analysis of the stained PBMC was performed by opt-distributed Stochastic Neighbor

Embedding (optSNE) dimensionality reduction followed by flowSOM consensus metaclustering using the cloud-based OMIQ data analysis software ([www.omiq.ai](http://www.omiq.ai)). The different cell populations were visualized and quantified.

**Immunohistochemical staining.** Formalin-fixed paraffin-embedded (FFPE) tumor tissues were used to cut 4 µm sections for immunohistochemical staining using antibodies against LRPAP1 (Merck HPA008001), HLA-class I (Nordic-MUBio HCA2 and HC10), beta globulin 2 (B2m; Abcam ERP21752-214), TAP 1 (Abcam EPR26236-57) and TAP2 (Abcam EPR26237-82). After deparaffinization, antigen retrieval was performed using Tris-EDTA (pH9) or Citrate (pH6) buffer (heated for 10 min). The tissue slices were blocked for 10–30 min at RT with SuperBlock blocking buffer (ThermoFisher) and incubated overnight with the primary antibodies indicated above. Next the slides were washed and incubated for 30 min with HRP-labeled secondary antibody, followed by color development using DAB (2–5 min; Agilent) and nuclear counter staining with Mayers Hematoxylin (15–30 s; Merck), rinsed with water to stop the staining, dehydration of the slides and mounting with Entellan (Merck) and covered with microscope cover slip (VWR).

**Statistical analysis.** Statistical data analysis was performed with Graphpad Prism V10.3.0 (Graphpad Software, LA Jolla, California, USA), R Software RStudio version 2024.04.2 and IBM SPSS Statistics version 28.0.1.0. The non-parametric Mann-Whitney U test (two-sided) was used when comparing two groups, whereas the non-parametric Kruskal-Wallis test (one-sided) with Dunn's multiple comparisons test was used when comparing >2 groups. Grouping patients based on highest detectable CD8 response was done by median (below or equal and/or above) or tertiles (i.e. lowest, middle and highest 33%) frequency of LRPAP1-specific CD8 + T cells as assayed by dextramer or ICS analysis, and on highest detectable CD4 response as assayed by ICS. To estimate the PFS and OS, Kaplan-Meier survival analysis was used. Wilcoxon signed rank tests (non-parametric, paired data) and Student's t test (parametric, paired data) were used to determine the statistical significance. Continuous variables were shown as median with the range of values or interquartile range (IQR). Categorical variables were presented as counts with percentages. Statistical significance was defined as p-values of 0.05 and below.

## Reporting summary

Further information on research design is available in the Nature Portfolio Reporting Summary linked to this article.

## Data availability

The data that support the findings of this study are not openly available due to reasons of sensitivity. Access to patient-level data is restricted due to data privacy laws. Access may be requested, and requests will be submitted to the central medical ethical regulatory committee to ensure that it is in line with lawful basis for processing, data protection regulations, and ethical standards. Upon approval, and completion of a data access agreement, access will be granted exclusively to qualified investigators for appropriate non-commercial use that is expected to lead to a publication. The processed de-identified immunology data are available under restricted access for privacy, ethical, and ongoing research concerns. Interested investigators can obtain and certify a data transfer agreement and submit requests by emailing the corresponding author ([shvdburg@lumc.nl](mailto:shvdburg@lumc.nl)). Responses to data requests will be provided within 30 days of receipt. Source data are provided with this paper.

## References

- Kalbasi, A. & Ribas, A. Tumour-intrinsic resistance to immune checkpoint blockade. *Nat. Rev. Immunol.* **20**, 25–39 (2020).
- Sharma, P., Hu-Lieskovan, S., Wargo, J. A. & Ribas, A. Primary, adaptive, and acquired resistance to cancer immunotherapy. *Cell* **168**, 707–723 (2017).
- Ren, Y. X. et al. Downregulation of expression of transporters associated with antigen processing 1 and 2 and human leukocyte antigen I and its effect on immunity in nasopharyngeal carcinoma patients. *Mol. Clin. Oncol.* **2**, 51–58 (2014).
- Kasajima, A. et al. Down-regulation of the antigen processing machinery is linked to a loss of inflammatory response in colorectal cancer. *Hum. Pathol.* **41**, 1758–1769 (2010).
- Bandoh, N. et al. HLA class I antigen and transporter associated with antigen processing downregulation in metastatic lesions of head and neck squamous cell carcinoma as a marker of poor prognosis. *Oncol. Rep.* **23**, 933–939 (2010).
- Seliger, B. et al. Association of HLA class I antigen abnormalities with disease progression and early recurrence in prostate cancer. *Cancer Immunol. Immunother.* **59**, 529–540 (2010).
- Tao, J. et al. Expression of transporters associated with antigen processing and human leukocyte antigen class I in malignant melanoma and its association with prognostic factors. *Br. J. Dermatol.* **158**, 88–94 (2008).
- Durgeau, A. et al. Human preprocalcitonin self-antigen generates TAP-dependent and -independent epitopes triggering optimised T-cell responses toward immune-escaped tumours. *Nat. Commun.* **9**, 5097 (2018).
- Leone, P. et al. MHC class I antigen processing and presenting machinery: organization, function, and defects in tumor cells. *J. Natl. Cancer Inst.* **105**, 1172–1187 (2013).
- Seremet, T. et al. Molecular and epigenetic features of melanomas and tumor immune microenvironment linked to durable remission to ipilimumab-based immunotherapy in metastatic patients. *J. Transl. Med.* **14**, 232 (2016).
- Doorduyn, E. M. et al. T cells specific for a TAP-independent self-peptide remain naive in tumor-bearing mice and are fully exploitable for therapy. *Oncoimmunology* **7**, e1382793 (2018).
- Doorduyn, E. M. et al. TAP-independent self-peptides enhance T cell recognition of immune-escaped tumors. *J. Clin. Investig.* **126**, 784–794 (2016).
- van Hall, T. et al. Selective cytotoxic T-lymphocyte targeting of tumor immune escape variants. *Nat. Med.* **12**, 417–424 (2006).
- Marijt, K. A. et al. Identification of non-mutated neoantigens presented by TAP-deficient tumors. *J. Exp. Med.* **215**, 2325–2337 (2018).
- Kenter, G. G. et al. Vaccination against HPV-16 oncoproteins for vulvar intraepithelial neoplasia. *N. Engl. J. Med.* **361**, 1838–1847 (2009).
- Melief, C. J. M. et al. Strong vaccine responses during chemotherapy are associated with prolonged cancer survival. *Sci. Transl. Med.* **12**, eaaz8235 (2020).
- Marijt, K. A., Griffioen, L., Blijleven, L., van der Burg, S. H. & van Hall, T. Cross-presentation of a TAP-independent signal peptide induces CD8 T immunity to escaped cancers but necessitates anchor replacement. *Cancer Immunol. Immunother.* **71**, 289–300 (2022).
- Garon, E. B. et al. Five-year overall survival for patients with advanced nonsmall-cell lung cancer treated with pembrolizumab: results from the phase I KEYNOTE-001 study. *J. Clin. Oncol.* **37**, 2518–2527 (2019).
- Korkolopoulou, P., Kaklamanis, L., Pezzella, F., Harris, A. L. & Gatter, K. C. Loss of antigen-presenting molecules (MHC class I and TAP-1) in lung cancer. *Br. J. Cancer* **73**, 148–153 (1996).
- Hilf, N. et al. Actively personalized vaccination trial for newly diagnosed glioblastoma. *Nature* **565**, 240–245 (2019).
- Keskin, D. B. et al. Neoantigen vaccine generates intratumoral T cell responses in phase Ib glioblastoma trial. *Nature* **565**, 234–239 (2019).



22. Ott, P. A. et al. An immunogenic personal neoantigen vaccine for patients with melanoma. *Nature* **547**, 217–221 (2017).
23. Ott, P. A. et al. A phase Ib trial of personalized neoantigen therapy plus anti-PD-1 in patients with advanced melanoma, non-small cell lung cancer, or bladder cancer. *Cell* **183**, 347–362.e324 (2020).
24. Sahin, U. et al. An RNA vaccine drives immunity in checkpoint-inhibitor-treated melanoma. *Nature* **585**, 107–112 (2020).
25. Besse, B. et al. Randomized open-label controlled study of cancer vaccine OSE2101 versus chemotherapy in HLA-A2-positive patients with advanced non-small-cell lung cancer with resistance to immunotherapy: ATALANTE-1. *Ann. Oncol.* **34**, 920–933 (2023).
26. Verdegaa, E. M. E. et al. Timed adoptive T cell transfer during chemotherapy in patients with recurrent platinum-sensitive epithelial ovarian cancer. *J. Immunother. Cancer* **11**, e007697 (2023).
27. Welters, M. J. et al. Vaccination during myeloid cell depletion by cancer chemotherapy fosters robust T cell responses. *Sci. Transl. Med.* **8**, 334ra352 (2016).
28. Pardieck, I. N. et al. A third vaccination with a single T cell epitope confers protection in a murine model of SARS-CoV-2 infection. *Nat. Commun.* **13**, 3966 (2022).
29. Rojas, L. A. et al. Personalized RNA neoantigen vaccines stimulate T cells in pancreatic cancer. *Nature* **618**, 144–150 (2023).
30. Sahin, U. et al. Personalized RNA mutanome vaccines mobilize poly-specific therapeutic immunity against cancer. *Nature* **547**, 222–226 (2017).
31. Marijt, K. A., Doorduijn, E. M. & van Hall, T. TEIPP antigens for T-cell based immunotherapy of immune-edited HLA class I(low) cancers. *Mol. Immunol.* **113**, 43–49 (2019).
32. Lee, S. J. et al. Pseudoprogression following neoadjuvant chemioimmunotherapy for lung squamous cell carcinoma mimicking pulmonary metastatic disease on computed tomography: A case report and review of the literature. *Radio. Case Rep.* **19**, 4029–4033 (2024).
33. Im, S. J. et al. Defining CD8+ T cells that provide the proliferative burst after PD-1 therapy. *Nature* **537**, 417–421 (2016).
34. Siddiqui, I. et al. Intratumoral Tcf1(+)PD-1(+)CD8(+) T Cells with Stem-like Properties Promote Tumor Control in Response to Vaccination and Checkpoint Blockade Immunotherapy. *Immunity* **50**, 195–211.e110 (2019).
35. Dammeijer, F. et al. The PD-1/PD-L1-checkpoint restrains T cell immunity in tumor-draining lymph nodes. *Cancer Cell* **38**, 685–700.e688 (2020).
36. Huang, A. C. et al. A single dose of neoadjuvant PD-1 blockade predicts clinical outcomes in resectable melanoma. *Nat. Med.* **25**, 454–461 (2019).
37. Oh, S. A. et al. PD-L1 expression by dendritic cells is a key regulator of T-cell immunity in cancer. *Nat. Cancer* **1**, 681–691 (2020).
38. Wu, T. D. et al. Peripheral T cell expansion predicts tumour infiltration and clinical response. *Nature* **579**, 274–278 (2020).
39. van Poelgeest, M. I. et al. Vaccination against oncoproteins of HPV16 for noninvasive vulvar/vaginal lesions: lesion clearance is related to the strength of the T-cell response. *Clin. Cancer Res.* **22**, 2342–2350 (2016).
40. Hu, Z. et al. Personal neoantigen vaccines induce persistent memory T cell responses and epitope spreading in patients with melanoma. *Nat. Med.* **27**, 515–525 (2021).
41. Saxena, M., van der Burg, S. H., Melief, C. J. M. & Bhardwaj, N. Therapeutic cancer vaccines. *Nat. Rev. Cancer* **21**, 360–378 (2021).
42. Hoos, A. et al. A clinical development paradigm for cancer vaccines and related biologics. *J. Immunother.* **30**, 1–15 (2007).

## Acknowledgements

We thank the patients and families for their unconditional trust and willingness to participate in our study. This study was funded by a

Clinical Proof of Concept grant (2019-0016) from the Oncode Institute to S.H.B., T.H. and J.G.A. We thank the OEDES team of the Oncode Institute for their help in the development of TEIPP therapy and for the initial design of this clinical trial in particular. The funder had no role in data collection and analysis or drafting of the manuscript. We thank our data safety monitoring board members J.R. Kroep, C.J.M. Melief and J. van Meerbeeck for their excellent support and advice.

## Author contributions

J.G.A. was the coordinating investigator. J.G.A. and H.G. were primary study investigators. T.H., J.G.A., S.H.B. contributed to the study design and development concept. M.E., M.V.D., E.F.S., D.W.D., A.L.G. and L.C.S. were clinical investigators of the study. M.E., M.V.D., J.G.A., T.H. and S.H.B. drafted the manuscript. M.J.P.W., S.J.S., S.B., A.S., N.M.L., N.F.C.C.M. and D.C. were responsible for laboratory studies. A.R.P.M.V. was responsible for vaccine design, production and management. All authors contributed to the acquisition, analysis or interpretation of (parts of the) data, and all performed critical revision of the manuscript for intellectual content.

## Competing interests

T.H. and S.H.B. have filed a patent on the TEIPP24 vaccine. None of the other authors have any competing interests.

## Ethics approval

This research aligns with the Inclusion & ethical guidelines embraced by Nature Communications.

## Additional information

**Supplementary information** The online version contains supplementary material available at <https://doi.org/10.1038/s41467-025-60281-8>.

**Correspondence** and requests for materials should be addressed to Sjoerd H. van der Burg.

**Peer review information** *Nature Communications* thanks the anonymous reviewer(s) for their contribution to the peer review of this work. A peer review file is available.












**Reprints and permissions information** is available at <http://www.nature.com/reprints>

**Publisher's note** Springer Nature remains neutral with regard to jurisdictional claims in published maps and institutional affiliations.

**Open Access** This article is licensed under a Creative Commons Attribution-NonCommercial-NoDerivatives 4.0 International License, which permits any non-commercial use, sharing, distribution and reproduction in any medium or format, as long as you give appropriate credit to the original author(s) and the source, provide a link to the Creative Commons licence, and indicate if you modified the licensed material. You do not have permission under this licence to share adapted material derived from this article or parts of it. The images or other third party material in this article are included in the article's Creative Commons licence, unless indicated otherwise in a credit line to the material. If material is not included in the article's Creative Commons licence and your intended use is not permitted by statutory regulation or exceeds the permitted use, you will need to obtain permission directly from the copyright holder. To view a copy of this licence, visit <http://creativecommons.org/licenses/by-nc-nd/4.0/>.

© The Author(s) 2025



**Mitchell Emmers** <sup>1,7</sup>, **Marij J. P. Welters** <sup>2,7</sup>, **Michelle V. Dietz**<sup>1,7</sup>, **Saskia J. Santegoets**<sup>2</sup>, **Sanne Boekesteijn**<sup>2</sup>, **Anouk Stolk**<sup>2</sup>, **Nikki M. Loof**<sup>2</sup>, **Daphne W. Dumoulin** <sup>1</sup>, **Annemarie L. Geel**<sup>1</sup>, **Lauri C. Steinbusch** <sup>3</sup>, **A. Rob P. M. Valentijn** <sup>4</sup>, **Danielle Cohen**<sup>5</sup>, **Noel F. C. C. de Miranda** <sup>5</sup>, **Egbert F. Smit**<sup>3</sup>, **Hans Gelderblom** <sup>6</sup>, **Thorwald van Hall** <sup>2</sup>, **Joachim G. Aerts** <sup>1</sup> & **Sjoerd H. van der Burg** <sup>2</sup> 

<sup>1</sup>Department of Pulmonary Medicine, Erasmus University Medical Center, Rotterdam, The Netherlands. <sup>2</sup>Department of Medical Oncology, Oncode Institute, Leiden University Medical Center, Leiden, The Netherlands. <sup>3</sup>Department of Pulmonary Disease, Leiden University Medical Center, Leiden, The Netherlands. <sup>4</sup>Department of Clinical Pharmacy and Toxicology, Leiden University Medical Center, Leiden, The Netherlands. <sup>5</sup>Department of Pathology, Leiden University Medical Center, Leiden, The Netherlands. <sup>6</sup>Department of Medical Oncology, Leiden University Medical Center, Leiden, The Netherlands. <sup>7</sup>These authors contributed equally: Mitchell Emmers, Marij J. P. Welters, Michelle V. Dietz. ✉e-mail: [shvdburg@lumc.nl](mailto:shvdburg@lumc.nl)